Single-chain folding and self-assembling of amphiphilic polyethyleneglycol-modified fluorinated styrene homopolymers in water solution

Elisa Guazzelli,[a] Elena Masotti,[a] Matteo Calosi,[a] Manfred Kriechbaum,[b] Frank Uhlig[b]*, Giancarlo Galli,[a] and Elisa Martinelli[a]*

[a] *Dipartimento di Chimica e Chimica Industriale and INSTM UdR Pisa, Università di Pisa, 56124 Pisa, Italy*

[b] *Institute for Inorganic Chemistry, Graz University of Technology, 8010 Graz, Austria*

Correspondence to: Elisa Martinelli (E-mail: elisa.martinelli@unipi.it) and Frank Uhlig (E-mail: frank.uhlig@tugraz.at)

Abstract

Amphiphilic tetrafluorostyrene monomers (EFSn) carrying in the *para* position a polyethyleneglycol (PEG) chain with varied lengths (n = 3–13) were synthesized and polymerized by ARGET-ATRP to obtain the corresponding amphiphilic homopolymers pEFSn-x with controlled and tailored polymerization degrees (x = 8–135). All polymers presented a reversible thermoresponsive LCST-type behavior, in water/methanol mixture when $n \leq 4$ or in pure water when $n \geq 8$, with a cloud point (C_p) temperature in the range 30–40 °C strictly dependent on the length of the PEG side chain. Combined small angle X-scattering (SAXS) and dynamic light scattering (DLS) measurements were used to study the self-assembly behavior in water of the water-soluble amphiphilic homopolymers. SAXS confirmed the formation of compact-sized and spherical single-chain self-folded nanostructures below C_p, that generally presented small hydrodynamic diameters ($D_h \leq 11$ nm) as proven by DLS analysis. Above C_p, much larger multi-chain aggregates were formed ($D_h \geq 800$ nm), that reversibly turned back to collapsed nanostructures on cooling below the C_p temperature. By contrast, the polymers were not able to self-assemble in THF or DMF solutions, in which they adopted conventional random coil conformations.

Keywords: single-chain nanoparticles, SAXS, amphiphilic polymer, thermoresponsive polymer, LCST

1 Introduction

Many natural macromolecules work as discrete objects with highly specific properties and functions deriving from a complex and well-defined chain structure capable under certain stimuli of self-assembling in the form required by such functions. As a contrast, synthetic polymer materials generally derive their properties from the collective behavior of a great number of macromolecular chains forming a myriad of intermolecular interactions that lead to the desired micro- and macro-scopic properties.

The synthesis of highly defined and functional three-dimensional structures with a monodisperse molecular weight distribution, such as natural polypeptide chains, remains beyond the reach of synthetic macromolecular chemistry. Nevertheless, a series of innovative approaches has led to alternative syntheses of polymers capable of self-assembling and forming compact nanosized functional three-dimensional structures. Such single chain polymer nanoparticles (SNCPs) can be obtained by reducing the conformational freedom of the macromolecular chain via various kinds of intramolecular interactions, both covalent and non-covalent[1–4]. While the initial syntheses of SCNPs used non-reversible reactions to obtain self-folding, there has been a growing focus on the self-assembling of the single polymeric chain through reversible folding. Such macromolecules have a stimuli-responsive and tunable character that more closely approaches the general characteristics of functional single-chain polymeric systems found in natural systems[3,5–9].

One such approach to reversible folding of SCNPs is through hydrophobic interactions, which provide a route to solvent-induced self-folding in aqueous solutions. The objects created by the folding of these polymers into more or less tightly segregated core-shell nanostructures, whose self-assembly mechanism resembles those of many natural macromolecules, have been termed unimer micelles for the first time in 1995[10]. The most common approach to obtain unimer micelles has thus far been the synthesis of amphiphilic random copolymers in which the hydrophilic and hydrophobic comonomers are statistically distributed along the polymeric backbone. Early research on unimer micelles was based on amphiphilic polyelectrolytes[10,11]; more recent work was instead concentrated on neutral random copolymers, in which the hydrophilic component is usually constituted by a oxyethylenic side-chain and the hydrophobic one may be chosen from a variety of lipo- or fluorophilic comonomers[12–19]. Among the interesting properties possessed by nanoobjects obtained from amphiphilic random copolymers are their stimuli-responsive nature, in particular their thermoresponsive solubility behavior in water or organic solvents, which may be regulated by varying comonomer ratio [17,20,21], the ability of controlling the size of the inner compartments[22–24], and the possibility of further using the single particles as building blocks for precision supramolecular nanostructures[25,26]. SCNPs based on hydrophobic interactions are also thought to be stable at higher concentrations and to possess a more globular structure when compared to classical covalently crosslinked SCNPs[27,28]. Possible applications for unimer micelles were explored in nanocatalysis[29–33], drug encapsulation and delivery[26,34,35] and as stabilizers for emulsion polymerization[36].

Amphiphilic homopolymers have been comparatively little studied as systems intrinsically able to self-fold in a selective solvent in a similar way to the one shown by amphiphilic random

copolymers. Amphiphilic homopolymer-based SCNPs have been obtained by grafting hydrophilic side-chains on a hydrophobic backbone[37]. In recent studies, polymers synthesized from double-brush type acrylates as amphiphilic monomers were found to be capable of self-folding into unimer micelles [38,39]. Pentafluorostyrene (PFS) could serve as the basic building block for such a homopolymer, as it is particularly well suited to modification by nucleophilic substitution, oriented preferentially to the *para* position, which can result in a diversity of functional groups being attached, such as groups carrying a hydrophilic functionality. The polymerization of pentafluorostyrene and its *para*-substituted monomers by atom transfer radical polymerization (ATRP) methods was reviewed and the base monomers were found to be as versatile as styrene, when it comes to polymerization conditions, and to contain vast potential for the creation of new materials when substituted[40]. The synthesis of an amphiphilic monomer using triethylene glycol as one such substituent has been thus far explored for the purposes of creating materials with anti-biofouling properties. The homopolymer was used as a component of block copolymers with poly(dimethyl siloxane) (PDMS) and PDMS-modified styrene finding that such systems were capable of undergoing comprehensive surface reconstruction after immersion in water and also displayed anti-biofouling properties[41,42]. A hyperbranched amphiphilic ATRP-prepared system featuring this substitution was also synthesized[43–45]. Although these amphiphilic PFS-based homopolymers were not water soluble, the self-assembly properties of aqueous solutions of copolymers of PFS and polyethylene glycol (PEG) methacrylate were investigated. While block copolymers formed multi-chain brush-type micelle aggregates[46,47], random copolymers formed substantially smaller nanostructures, although these structures were still considered to be supramolecular aggregates[48]. The thermoresponsive properties of these random copolymers were exploited for the removal of organic dyes from water through encapsulation[49].

In this work we designed and synthesized new PFS-derived amphiphilic homopolymers, named pEFSn-x, in which the effects of the hydrophobic fluorostyrene backbone and the hydrophilic PEG side chain substituent were inherently mixed and partly offset with each other. This was aimed at creating an amphiphilic polymer system that would be selectively soluble in water and capable of reversibly self-folding in dynamic single-chain nanostructures, which in addition could self-assemble in multi-chain nanostructures as a response to temperature. The details of the self-folding and self-assembling were found to depend on the number n of oxyethylene units in the PEG side chains and the average number degree of polymerization x of the polymer. Small-angle X-ray scattering (SAXS) measurements revealed the existence of compact-sized and spherical single-chain self-folded nanostructures in water solutions below a cloud point transition temperature, that exhibited small hydrodynamic diameters ($D_h \leq 11$ nm) as proved by dynamic light scattering (DLS) analysis. Above such temperature, much larger multi-chain aggregates were formed, that in fact reversibly turned back to nanostructures on cooling below the cloud point temperature.

2 Experimental section

2.1 Materials

2,3,4,5,6-Pentafluorostyrene (PFS) (Fluorochem), triethylene glycol monomethyl ether (mPEG3), tetraethylene glycol monomethyl ether (mPEG4), poly(ethylene glycol) monomethyl ether (mPEG8, M_n = 350 g/mol, $Đ$ (= M_w/M_n) = 1.12), poly(ethylene glycol) monomethyl ether (mPEG13, M_n = 550 g/mol, $Đ$ = 1.12), tin(II) 2-ethylhexanoate ($Sn(EH)_2$) (Sigma-Aldrich) were used as received. Anisole (Sigma-Aldrich) was vacuum distilled over sodium, tetrahydrofuran (Sigma-Aldrich) was refluxed over CaH_2 and then distilled under nitrogen, *N*,*N*′,*N*′′,*N*′′-pentamethyldiethylenetriamine (PMDTA) and (1-bromoethyl) benzene (1-BEB) (Sigma-Aldrich) were vacuum distilled. $CuBr_2$ (Sigma-Aldrich) was recrystallized from water solution. Common laboratory solvents and other reagents (Sigma-Aldrich) were used as received.

2.2 Synthesis of monomers EFSn

The monomers synthesized were named EFSn, where n stands for the number of repeat units in the mPEGn chain.

EFS3 (M_n = 380 g/mol, $Đ$ = 1.03) and EFS4 (M_n = 470 g/mol, $Đ$ = 1.03) monomers were prepared and purified via similar procedures, described herein for EFS4. In a typical preparation a NaH 60 wt% dispersion in mineral oil (0.72 g, 18 mmol) was slowly added under N_2 to a solution of mPEG4 (3.66 g, 17.60 mmol) in anhydrous THF (30 mL) at 0 °C. The solution was stirred for 30 minutes, then PFS (3.56 mL, 26.3 mmol) dissolved in 10 mL of anhydrous THF was slowly added. The reaction was conducted at 0 °C and under N_2 for an additional 4 h. The reaction mixture was then concentrated under vacuum, dissolved in ethyl acetate and washed twice with deionized water. The resulting organic phase was dried over anhydrous $MgSO_4$ and evaporated to dryness under vacuum, obtaining a pale yellow oil. The crude product was further purified by flash chromatography on silica gel using ethyl acetate/dichloromethane (50/50 v/v) as eluent. The final product (yield 63%) was characterized by ^{1}H and ^{19}F NMR analyses (Figures S1-S4).

^{1}H NMR (chloroform-d): δ (ppm) = 6.64 (dd, *J* = 18.0, 11.9 Hz, 1H, =C**H**), 6.04 (d, *J* = 18.0 Hz, 1H, **H**(H)C=CH), 5.65 (d, *J* = 11.9 Hz, 1H, **H**(H)C=CH), 4.40 (t, *J* = 4.5 Hz, 2H, $ArOCH_2$), 3.9–3.5 (m, 14.8H, OCH_2), 3.39 (s, 3H, OCH_3).

^{19}F NMR (chloroform-d, hexafluorobenzene): δ (ppm) = –145.11 (dd, *J* = 20.6, 8.4 Hz, 2F *meta*), –158.04 (dd, *J* = 20.6, 8.4 Hz, 2F *ortho*).

EFS8 (M_n = 750 g/mol, $Đ$ = 1.08) and EFS13 (M_n = 1100 g/mol, $Đ$ = 1.09) monomers were prepared and purified via similar procedures, described herein for EFS13. In a typical preparation a NaH 60 wt % dispersion in mineral oil (0.40 g, 10 mmol) was slowly added under N_2 to a solution of mPEG13 (4.56 g, 7.67 mmol) in anhydrous THF (40 mL) at 0 °C. The solution was stirred for 30 minutes, then PFS (1.72 mL, 12.4 mmol) dissolved in 5 mL of anhydrous THF was slowly added. The reaction was conducted at 0 °C under N_2 for an additional 5 h. The reaction mixture was then concentrated under vacuum, dissolved in deionized water and washed with petroleum ether. The aqueous phase was then washed with ethyl acetate and the combined organic phases were dried over anhydrous $MgSO_4$, passed through a neutral

alumina column and evaporated to dryness under vacuum, obtaining a colorless viscous oil. The final product (yield 80%) was characterized by ^{1}H and ^{19}F NMR analyses (Figures S5-S8).

^{1}H NMR (chloroform-d): δ (ppm) = 6.61 (dd, *J* = 18.0, 11.92 Hz, 1H, =C**H**), 6.02 (d, *J* = 18.0 Hz, 1H, **H**(H)C=CH), 5.62 (d, *J* = 11.9 Hz, 1H, **H**(H)C=CH), 4.36 (t, *J* = 4.5 Hz, 2H, ArOC**H₂**), 3.9–3.5 (m, 50.4H, OCH_2CH_2O), 3.39 (s, 3H, OCH_3)

^{19}F NMR (chloroform-d, hexafluorobenzene): δ (ppm) = –145.08 (dd, *J* = 20.7, 8.4 Hz, 2F *meta*), –158.02 (dd, *J* = 20.7, 8.4 Hz, 2F *ortho*)

2.3 Synthesis of homopolymers pFSn-x

The polymers synthesized were named pFSn-x, where n stands for the number of repeat units in the mPEG side chain and x for the number of repeat units (number average degree of polymerization) in the homopolymer.

The general procedure was identical for each polymerization reaction. The preparation of homopolymer pEFS3-46 is described as a typical example. A 0.0134 M solution of the $CuBr_2$/PMDTA complex (0.001 mmol) in methanol (3 g/L of $CuBr_2$) was introduced in a Carius tube and then dried under vacuum for 1 h. EFS3 (0.699 g, 2.07 mmol), 1-BEB (4.7 µL, 0.034 mmol) and anisole (1.4 mL) were then added, and the mixture was degassed with three freeze-pump-thaw cycles. Then $Sn(EH)_2$ (1.4 mg, 0.0034 mmol) and PMDTA (0.7 µL, 0.0034 mmol) in 0.1 mL of anisole were added and three more freeze-pump-thaw cycles were performed. The polymerization was conducted at 110 °C under vacuum and with magnetic stirring for 21 h. The reaction was stopped by exposure to air and quenching to room temperature. The crude product was precipitated three times from chloroform solutions into n-hexane, then dissolved in chloroform and passed through a neutral alumina column. After drying under vacuum, the final product (yield 72%) was characterized by ^{1}H (Figure S9), ^{19}F NMR (Figure S10) and GPC analyses.

^{1}H NMR (acetone-d_6): δ (ppm) = 6.9–7.2 (5H, aromatic), 5.0–5.3 (1H, ArC**H**Br), 4.2–4.4 (92H, ArOC**H₂**), 3.4–3.9 (478H, OCH_2), 3.39 (138H, OCH_3), 1.8–3.1 (138H, $CHCH_2$).

^{19}F NMR (chloroform-d, hexafluorobenzene): δ (ppm) = –142.2 to –146.1 (2F *meta*), –155.9 to –158.02 (2F *ortho*)

GPC: M_n = 10700 g/mol, $Đ$ = 1.23.

2.4 Characterization

^{1}H and ^{19}F NMR measurements were carried out on a Bruker Avance 400 (400 MHz) spectrometer with deuterated solvents at room temperature. Sample concentration was approximately 30 g/L. For attribution of ^{19}F NMR chemical shifts, hexafluorobenzene was used as an internal standard, to which a shift of –161.64 ppm in $CDCl_3$ was assigned compared to $CFCl_3$. For ^{1}H spectra the internal standard was the solvent peak.

The number and weight average molecular weights (M_n, M_w) were determined by gel permeation chromatography (GPC), using a Jasco PU-2089 Plus liquid chromatograph equipped with two PL gel 5 µm mixed-D columns, a Jasco RI-2031 Plus refractive index detector and a Jasco UV-2077 Plus UV/vis detector. Measurements were carried out using chloroform as the mobile phase, at a flux of 1 mL/min and a temperature of 30 °C maintained by a Jasco CO 2063 Plus column thermostat. Polystyrene standards were used for calibration. Samples were filtered with a 0.2 µm PTFE filter before injection.

UV/vis measurements were carried out using a Perkin-Elmer Lambda 650 and a Shimadzu 2450 spectrophotometers. Solution samples were put in quartz cuvettes with a 10 mm optical path. Light transmittance was measured as a function of temperature at a fixed wavelength of 700 nm and a cloud point (C_p) temperature was determined when transmittance dropped to 50%. Temperature was varied manually using a thermostat.

DLS measurements of polymer solutions were taken with a Malvern Zetasizer Nanoparticle analyzer (detection angle = 173°). Intensity, volume and number distributions were obtained from the signal autocorrelation function through CONTIN analysis in the instrument software. Samples were prepared using solvents of the highest available purity grade that were previously filtered through 0.2 µm PTFE (organic solutions) or cellulose acetate (water solutions) filters in order to reduce external contamination. After dissolving the chosen substance, the solutions were then filtered through 5 µm PTFE or cellulose acetate filters. At least 5 separate measurements were carried out for each solution. When all the results were coherent with each other, an instrument software-created average size distribution curve was considered as an overall representative of the system.

Small angle X-ray scattering (SAXS) studies were performed using an Anton Paar SAXSess system (Anton Paar, Austria) equipped with a temperature-controlled sample cell. The X-ray source, a Debyeflex 3003 X-ray generator (GE-Electric, Germany), was operated at 40 kV and 50 mA with a sealed-tube Cu anode (Cu-K_α radiation source with λ = 0.154 nm). The X-ray beam was rectangularly shaped (17 mm horizontal and 0.25 mm vertical dimensions at the sample) after being Goebel-mirror focused and Kratky-(line) slit collimated. Spectra were recorded in transmission mode by a one-dimensional MYTHEN-1k microstrip solid-state detector (Dectris, Switzerland), within a q range of 0.01–5 nm^{-1}, with q being the magnitude of the scattering vector. The sample-to-detector distance of 307 mm corresponded to a total 2θ region of 0.14°–7° applying the conversion $q = 4\pi\sin(\theta)/\lambda$ with 2θ being the scattering angle with respect to the incident beam and λ the wavelength of the X rays. The sample cell in the X-ray beam was a quartz capillary (1 mm diameter, 10 µm wall thickness), sealed by vacuum-tight screw-caps on both ends. Vacuum during the measurements was ~ 1 mbar. The exposure time was typically 60 s times 5 with a waiting time of 10 min between different temperature steps for all spectra. 20 g/L water solutions were investigated to warrant enough SAXS intensity for analysis. The background (pure solvent) intensity was recorded separately and subtracted from all recorded SAXS curves.

3 Results and Discussion

3.1 Syntheses

Amphiphilic homopolymers based on a fluorinated styrene backbone carrying polyethyleneglycol (PEG) pendant chains in the *para* position were synthesized. In order to obtain amphiphilic polymers with a varying degree of hydrophobicity, four different monomers were used, named EFSn, where n describes the number of oxyethylene repeat unit in the side chains (n = 3, 4, ~8, and ~13) (Figure 1). A literature procedure for the synthesis of EFS3[41,43,44] had to be optimized for the synthesis of the present monomers at lower reaction temperatures without formation of unwanted byproducts.

The homopolymers were prepared by activators regenerated by electron transfer-atom transfer radical polymerization (ARGET-ATRP), using 1-BEB as initiator, $CuBr_2$ as catalyst, PMDTA as ligand, $Sn(EH)_2$ as reducing agent and anisole as solvent at 110 °C, operating either under a nitrogen atmosphere or under vacuum (Figure 1). To study the effect of polymer chain length on self-assembly, we prepared for each monomer a set of homopolymer samples, identified as pEFSn-x, where x is the number average degree of polymerization of the polymer. Owing to the controlled nature of the polymerization procedure adopted, x could be largely varied and well tuned over a wide range of values (x = 8–135). The success of polymerization was confirmed by ^{1}H NMR and ^{19}F NMR analyses (Figures S9-S13). Moreover, polymers were typically characterized by monomodal GPC curves with narrow dispersity of molecular weights (*Đ* = 1.1–1.3) (Figure S14), although the ones starting from EFS8 and EFS13 were more distributed (*Đ* = 1.4–2.3), due to dispersity of the two monomers themselves (Table 1).

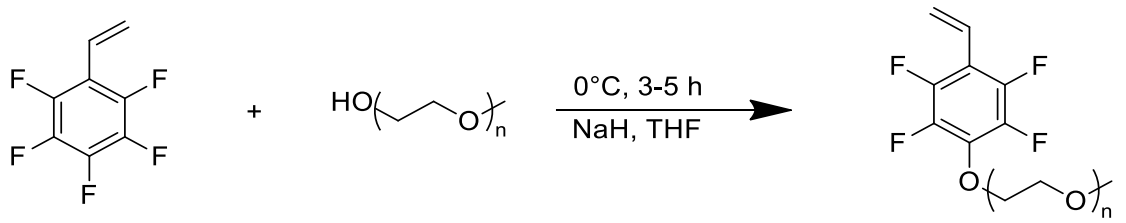

PFS mPEGn n = 3, 4, 8, 13 EFSn

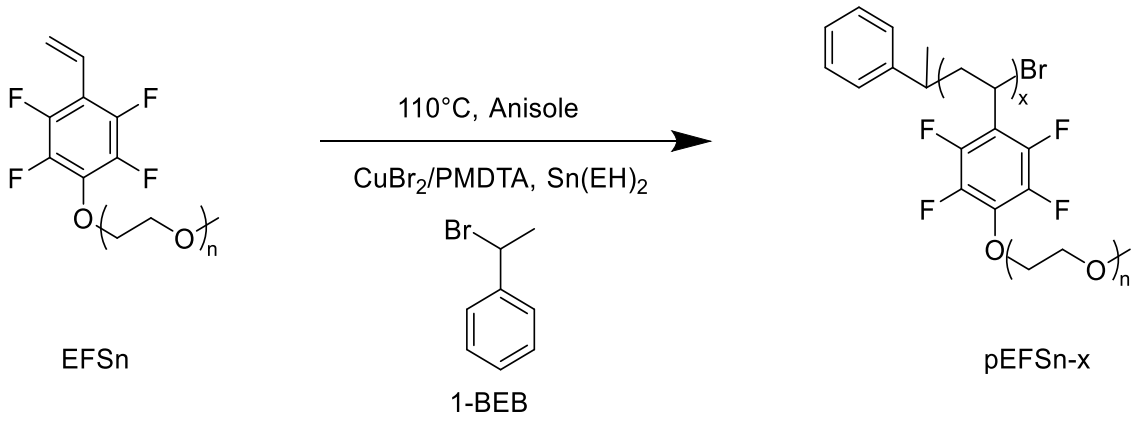

Figure 1: Reaction schemes for the synthesis of monomers EFSn and respective homopolymers pEFSn-x

Table 1: Physico-chemical characteristics of polymers pEFSn-x

Polymer[a]	***Atmosphere***	***M/I ratio[b]***	***Conversion (%)***	***x***	***M_n[c] (g/mol)***	***M_n[d] (g/mol)***	***Đ[e]***
pEFS3-17	N_2	25	55	17	5750	4400	1.14
pEFS3-28	N_2	50	50	28	9470	6400	1.23
pEFS3-46	Vacuum	60	92	46	15560	10700	1.23
pEFS4-17	Vacuum	15	90	17	6360	6000	1.15
pEFS4-22	Vacuum	30	83	22	8230	6100	1.18
pEFS4-53	Vacuum	60	94	53	19830	13000	1.28
pEFS8-16	Vacuum	15	95	16	8870	9800	1.17
pEFS8-26	N_2	24	99	26	14410	10800	1.26
pEFS8-46	Vacuum	60	93	46	25490	19800	1.25
pEFS8-72	Vacuum	200	60	72	39900	34700	1.31
pEFS8-135	Vacuum	120	90	135	74800	35800	1.53
pEFS13-8	Vacuum	6	95	8	6150	9100	1.42
pEFS13-25	Vacuum	25	96	25	19200	15100	1.37
pEFS13-46	Vacuum	60	90	46	35330	30200	2.30
pEFS13-54	Vacuum	60	85	54	41480	23400	1.75

[a] *Polymers were synthesized with an initiator/$Sn(EH)_2$/$CuBr_2$/PMDETA mole ratio of 1/0.1/0.03/0.13.*

[b] *Monomer/initiator mole ratio.*

[c] *Number average molecular weight by ^1H NMR.*
[d] *Number average molecular weight and dispersity by GPC.*

3.2 Solubility of monomers and polymers

The solubility in water at room temperature of monomers EFSn and polymers pEFSn-x was tested. For substances insoluble in water we then tried to find the least proportion of a less polar water-miscible cosolvent (methanol) which led to full solubility of the chosen sample. Only the monomers with longer PEG chains (≥ 8), as well as their respective polymers were fully soluble in water. All samples proved to be soluble in methanol and required different proportions of methanol as a cosolvent with water to become soluble in a water/methanol mixture. Such a solution was considered the most polar medium in which these substances could be solvated and was as such later used to study their self-assembly and thermoresponsive solubility. The quantity of methanol needed to achieve solubility was found to decrease with increasing PEG chain length, e.g. 50–55 vol% for polymers pEFS3 (Table 2).

Table 2: Solubility properties of monomers and polymers in water or water/methanol

Sample	*Water soluble*	*Methanol proportion (vol%)*
EFS3	–	40
EFS4	–	35
EFS8	+	
EFS13	+	
pEFS3-x	–	50–55
pEFS4-x	–	25–30
pEFS8-x	+	
pEFS13-x	+	

PEG-based amphiphilic polymers commonly display thermoresponsive solubility in water with a lower critical solution temperature (LCST)[50,51] behavior. Thus, the cloud points (C_p) of the water and water/methanol solutions of homopolymers pEFSn-x were determined by temperature-dependent UV/vis measurements, where the transmittance of the solutions of visible light was monitored at λ = 700 nm by changing temperature. The cloud point was defined as the temperature at which the transmittance became 50% of the original one upon heating. For the water-insoluble polymers two different C_ps were identified; the first one was determined by a water/methanol solution in which the minimum amount of methanol co-solvent was added to solubilize the polymer, while the second one was obtained by solubilizing the polymer in a water/methanol solution containing the same volume percentage of co-solvent (55 vol%) (Table 3). The latter experiment was more indicative of the effect of the PEG side chain length on the C_p. Results indicate that while pEFS3-x copolymers exhibited a C_p, pEFS4-x copolymers, containing one more oxyethylenic unit in the side chain, did not show a

LCST transition, given their higher hydrophilicity. Moreover, for pEFS3-x of the same set, C_p was found to increase with increasing polymerization degree of the polymers.

Water-soluble monomers EFS8 and EFS13 and their corresponding homopolymers displayed a thermoresponsive behavior, with a sharp LCST-like transition to cloudy dispersions in all cases (Table 3). Some differences in temperature (7–9 °C) were noticed in the exact location of C_p for the polymers of the same set with different degrees of polymerization, but there was no clear trend where C_p varied along with chain length. A trend was observed in water-soluble polymers, for which the thermal transition happened at significantly higher temperatures than in the corresponding monomers. In both monomers and polymers, the presence of a longer PEG side chain resulted in a higher C_p (Table 3). This is analogous to the behavior of PEG methacrylate polymers with varying length of PEG side chain[50]. Thus, it is expected that polymers pEFSn with longer PEG side chains will not show a LCST in water at standard pressure. The thermoresponsive behavior was also found to be reversible as shown in Figure 2 for pEFS8-26 taken as an illustration. The phase-transition reversibility was also recently proved by calorimetric investigations[52]. While a few examples of thermoresponsive copolymers of PFS and PEG methacrylate are known[41], the present amphiphilic homopolymers seem to be the first examples of mixed fluorinated-PEGylated homopolymers that are able to differently self-assemble with a reversible response to temperature in water solution.

Table 3: Cloud point temperatures of monomer and polymer solutions (5 g/L), in water unless otherwise noted

Sample	***C_p (°C)***	
EFS8	33	
EFS13	34	
pEFS3-17[a]	38[a]	38[e]
pEFS3-28	39[b]	50[e]
pEFS3-46	37[b]	55[e]
pEFS4-17	31[c]	n.d.[e]
pEFS4-22	34[d]	-
pEFS4-53	38[d]	n.d.[e]
pEFS8-16	72	
pEFS8-26	69	
pEFS8-46	72	
pEFS8-72	78	
pEFS8-135	73	
pEFS13-8	86	
pEFS13-25	92	
pEFS13-46	85	

[a]55 vol% methanol as co-solvent.
[b]50 vol% methanol as co-solvent.
[c]30 vol% methanol as co-solvent.
[d]25 vol% methanol as co-solvent.
[e]55 vol% methanol as co-solvent.

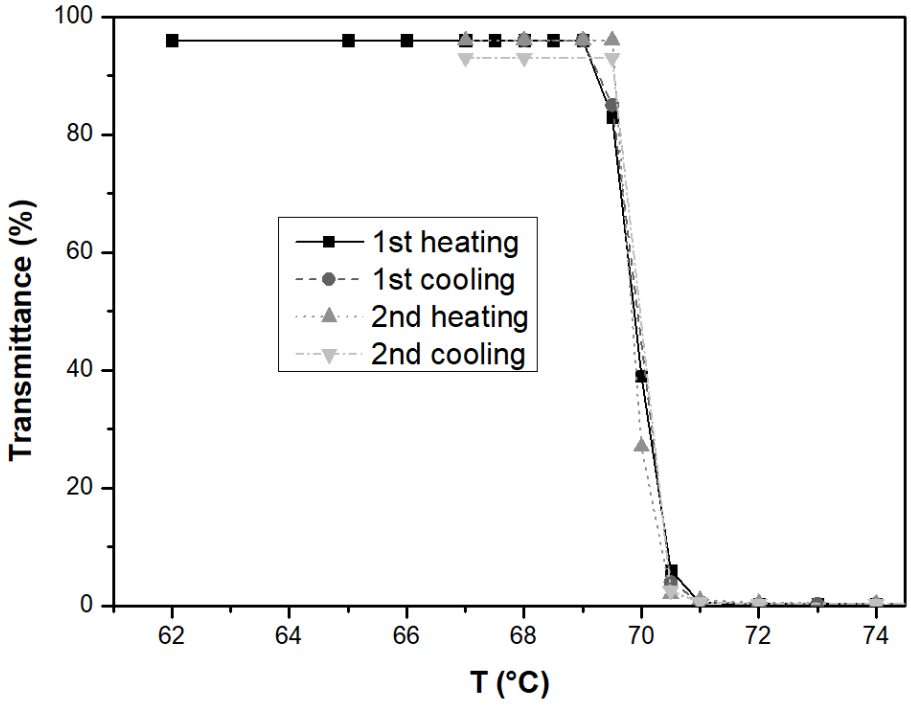

Figure 2. Light transmittance of water solutions (5 g/L) of pEFS8-26 as a function of temperature.

3.3 Single-chain folding and self-assembling

3.3.1 DLS investigation

DLS measurements were performed on monomer and polymer solutions by changing solvent, concentration, and temperature, to evaluate their ability to spontaneously single-chain fold in a suitable solvent. For each sample, 5 g/L (unless otherwise stated) solutions in water or organic solvents were prepared. Solutions were analyzed at 25 °C and at a temperature above C_p. pEFS13 polymers could not be analyzed above C_p because of instrumental temperature limitations.

The water-soluble monomers (EFS8 and EFS13) were found to form particles with a hydrodynamic diameter (D_h) of several hundred nanometers, significantly larger for EFS13 compared to EFS8 (Table 4) (Figures S15 and S17). This confirms the formation of classical aggregate micelles. Past C_p, both monomers were found to form larger, micron-sized aggregates (Figures S16 and S18).

Table 4: DLS hydrodynamic diameter distribution for water-soluble monomers

Monomer	$D_h^{(T=25°C)}$	$D_h^{(T>Cp)}$
EFS8	160 ± 60	1300 ± 500
EFS13	500 ± 200	1100 ± 200

Water and water/methanol solutions of polymers presented in all cases a bimodal intensity size distribution at room temperature, with a population with a smaller D_h (generally less than 10 nm) and a population with a much larger D_h (hundreds of nm), as shown in Figure 3 for polymer pEFS8-72, as a typical illustration. The former is consistent with the existence of self-folded single-chain polymers, while the latter is ascribed to the formation of multi-chain aggregates, which were difficult to dissolve at a molecular level. However, it was evident that the predominant form in solution was the single-chain folded particles, that accounted for at least 98% of particle volume in the volume distribution (Figure 3). This kind of bimodal size distribution was reported for the self-assemblies of amphiphilic random copolymers containing fluorinated elements[13,14].

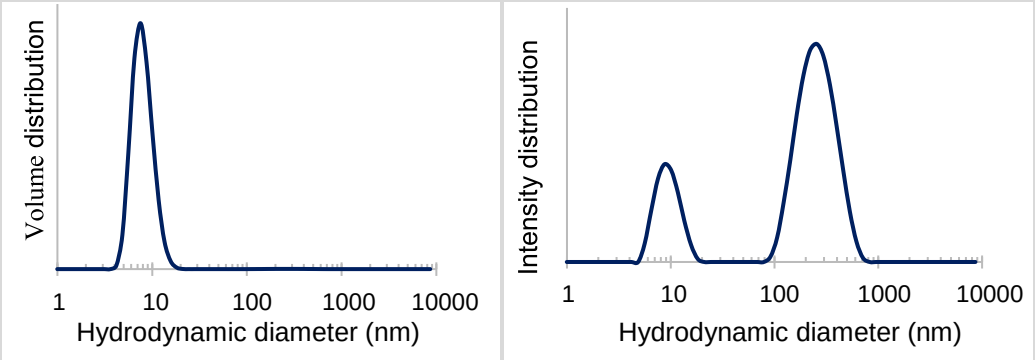

Figure 3: DLS volume (left) and intensity (right) distribution for pEFS8-72 in water solution (5 g/L) at 25 °C

At room temperature water soluble polymers generally exhibited a D_h comprised between 6 and 11 nm (Table 5) (Figures S19, S21, S23 and S25). The evaluated D_h was compatible with diameters determined for so-called unimer micelles formed by the self-assembly in water of amphiphilic PEG-containing random copolymers[12,13,15]. Their existence in water solution was confirmed by SAXS measurements, as discussed below. Self-assembly in water/methanol solution for the water insoluble polymers was found to lead to the formation of similarly sized particles, probably deriving from the same type of nanostructuring in what was still a very polar protic solvent. Particle size tended to slightly increase with increasing degree of polymerization within sets of polymers obtained from the same monomer, notably that with longest PEG side chain.

When measured at temperatures above C_p, particle diameter was in all cases above 800 nm (Table 5) owing to the formation of much larger multi-chain particles (Figures S20, S22 and S24). This was due to the aggregation of multiple polymer chains at such temperature where hydrophilic polymer–water interactions were no longer capable of solvating individual single-

chain particles and hydrophobic polymer–polymer interactions became predominant. These multi-chain aggregates generally presented a D_h between 800 and 1800 nm with a narrow, monomodal distribution. However, in a few cases a further aggregation behavior was noticed, with the occurrence of even larger particles (D_h > 2 µm) within a bimodal distribution. This was likely caused by additional coalescence of multi-chain aggregates with each other. No clear correlation between polymer structure and aggregate coalescence appeared (Table 5).

Table 5: DLS average hydrodynamic diameters of polymer solutions (5 g/L), in water unless otherwise noted

Homopolymer	$D_h^{(T=25\ °C)}$ ***(nm)***	$D_h^{(T>Cp)}$ ***(nm)***
pEFS3-17[a]	5 ± 1	800 ± 100
pEFS3-28[b]	5 ± 1	1800 ± 700
pEFS3-46[b]	7 ± 2	Bimodal
pEFS4-17[c]	7 ± 2	900 ± 300
pEFS4-22[d]	7 ± 1	1200 ± 300
pEFS4-53[d]	6 ± 2	1100 ± 300
pEFS8-16	6 ± 1	1800 ± 300
pEFS8-26	6 ± 1	Bimodal
pEFS8-46	7 ± 2	1500 ± 300
pEFS8-72	10 ± 2	Bimodal
pEFS8-135	11 ± 4	1800 ± 400
pEFS13-8	6 ± 1	-
pEFS13-25	7 ± 2	-
pEFS13-46	30 ± 20	-

[a] 55 vol% methanol as co-solvent.
[b] 50 vol% methanol as co-solvent.
[c] 30 vol% methanol as co-solvent.
[d] 25 vol% methanol as co-solvent.

Polymer pEFS8-46 was selected to test the effect of polymer concentration (0.5, 5, 10, and 20 g/L) in water on self-assembly. At 25 °C no appreciable size difference was detected for the different concentrations (D_h ~7–8 nm). At 80 °C, past C_p, the multi-chain aggregates changed size from D_h = 300 nm at 0.5 g/L to 1500 nm at 5 g/L and to even larger (> 2000 nm) at higher concentration. Thus, formation of single-chain particles was not influenced by concentration in the range measured, whereas the coalescence of multi-chain particles depended on concentration, with larger aggregates being formed gradually as polymer concentration increased. These findings evidenced the distinct unimolecular and multimolecular characters of the former and the latter assemblies, respectively. The tendency of the polymer to assemble spontaneously in organic and mixed water/organic solutions (5 g/L) was investigated. Determined values of D_h are reported in Table 6, compared to water for reference.

Table 6: Hydrodynamic diameter of pEFS8-46 in various solutions

Solvent	***H_2O***	***DMF***	***$CHCl_3$***	***THF***
D_h (nm)	7 ± 2	10 ± 4	8 ± 2	8 ± 2

Particle size was found to be larger in any organic solvent used than in water. While the dimensions were compatible with those of single polymeric chains, the polymer was arranged in more sparse, random coil conformations.

3.3.2 SAXS investigation

The formation in water solution of single-chain, self-folded nanostructures at temperatures below C_p and their morphology were investigated by small angle X-ray scattering (SAXS). Measurements on water-soluble amphiphilic homologue polymers pEFS-8 and pEFS-13 (20 g/L water solution) were also recorded at various temperatures. The scattering intensity profile of pEF8-46 in water as a function of the scattering vector *q*, after proper background subtraction of the pure solvent (water), is shown in Figure 4 as a representative example.

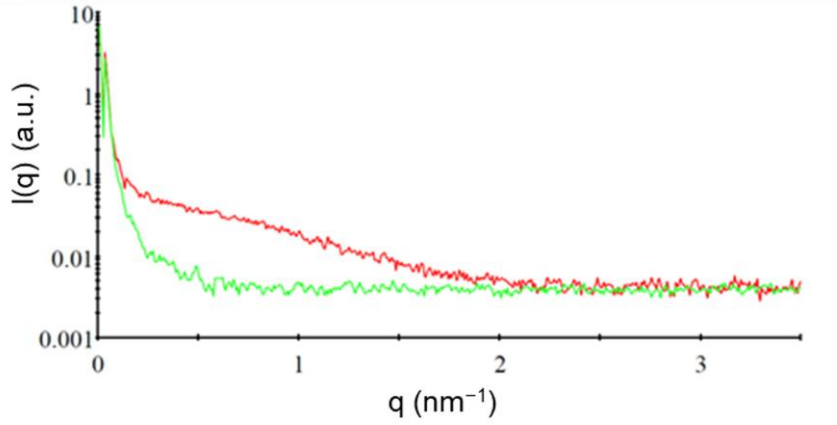

Figure 4: Scattering intensity of pEFS8-46 in water solution (20 g/L) (red) and water (green) at 25 °C

Measured SAXS intensity data were reported in a Guinier plot in the region of low *q* values as ln *I*(*q*) vs q^2 (Figure 5). Linearity of the Guinier plot towards $q = 0$ indicated the existence of non-aggregated and monodisperse assemblies. At room temperature no interactions occurred among the particles in solution.

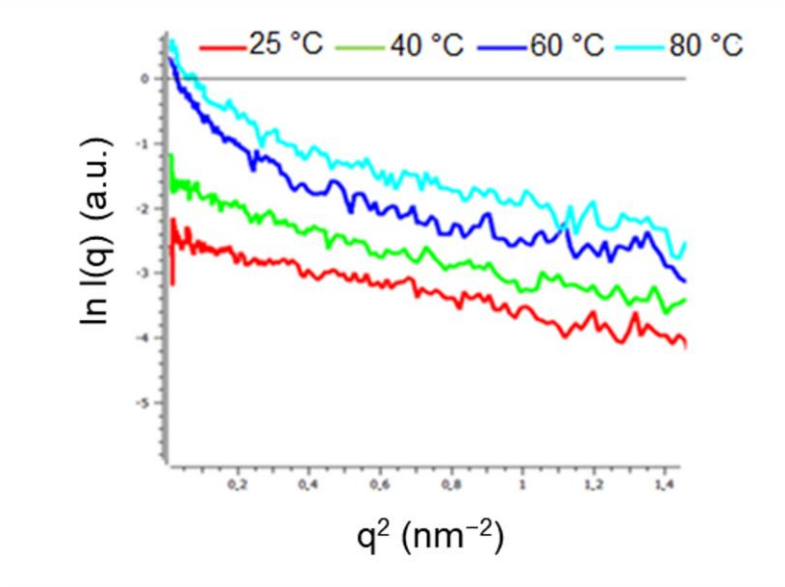

Figure 5: Guinier plots of pEFS8-46 in water solution (20 g/L) at various temperatures

On increasing the temperature, linearity of scattering curves was lost in the Guinier region. This change was due to the onset of intermolecular interactions among the polymer chains in the water solution. A positive deviation from linearity of scattering intensity in the Guinier region is attributed to an attractive aggregation phenomenon, while a negative deviation from linearity is ascribed to repulsive interactions[51]. All analyzed samples in water solution showed the same behavior with a positive deviation from linearity indicating the existence of attractive force due to polymer-polymer hydrophobic interactions. The radius of gyration (R_g) of the particles (which is proportional to the size of the particles) was obtained by a linear fit of the Guinier (low q) region. An account of determined values of R_g for the analyzed polymers and their variation with temperature is reported in Table

Table 7: Values of radius of gyration (R_g) of polymers *pEFS8-46, pEFS8-135, pEFS13-8 and pEFS13-46* as evaluated by SAXS

Polymer	***R_g (nm)***	***T (°C)***
pEFS8-46	1.5 ± 0.1	20
	1.3 ± 0.2	40
	1.8 ± 0.2	60
	2.0 ± 0.2	65
pEFS8-135	1.4 ± 0.1	40
	1.6 ± 0.2	60

	2.0 ± 0.1	65
pEFS13-8	1.66 ± 0.03	40
	1.75 ± 0.02	60
	1.86 ± 0.04	75
	2.11 ± 0.03	80
	2.39 ± 0.03	83
pEFS13-46	1.89 ± 0.06	40
	1.89 ± 0.07	60
	2.19 ± 0.07	70
	2.33 ± 0.07	75
	2.56 ± 0.08	80

All polymers exhibited a plateau region for the value of R_g which stayed mostly stable over a range of temperatures. A few degrees below C_p the radius started to increase markedly, and instrumental resolution lost reliability when C_p was reached. Evaluation of actual R_g of the multi-chain aggregates above C_p temperature could not be performed. The ratio between the values of SAXS radius of gyration and DLS hydrodynamic radius R_g/R_h was found to be quite low (< 0.5), with predicted values varying from 0.778 for spheres[53] to 1.16 for random coils[54]. This is attributed to the dense core-shell structure with different electron densities of the particles, with the hydrophilic shell being swollen by the selective solvent.[55,56] The core-shell structure was confirmed by fitting the scattering curve of the copolymer pEFS8-46 in water at 20 °C in the range $0.3 < q < 3$ nm^{-1} (Figure 6b), with a spherical core-shell model [57] using the program SasView (www.sasview.org). The fitting parameters were the core radius, the thickness of the shell and the electron density core/shell ratio (with respect to water), allowing the core and shell radii to have a polydisperse Schulz size distribution. The best fit obtained resulted in a core radius of r = 0.63 nm with a very narrow distribution and a shell thickness of 1.69 nm with a broader distribution centered at r = 2.32 nm (core + shell thickness) as illustrated in Figure 6a. The core/shell ratio of their respective electron densities was 15.5/1 (i.e. the electron density of the core is 15.5 times higher than that of the shell). Fitting at higher temperatures was not reliable due to increasing aggregation.

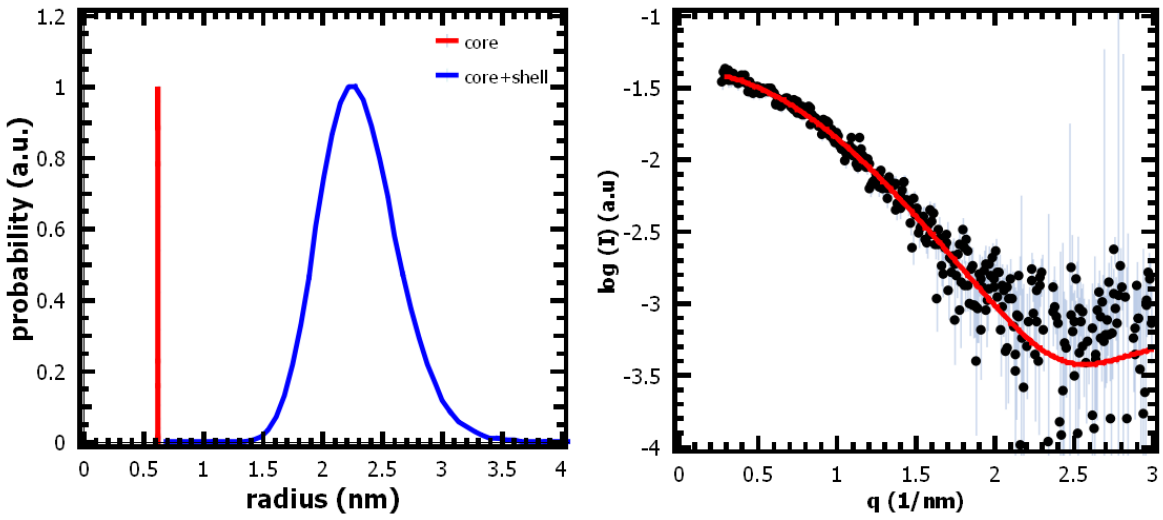

(a) (b)

Figure 6: Core-shell model of pEFS-46 in water at 20 °C (a) obtained from a fit of the experimental SAXS-data (red: fit, black: experimental data) (b).

The real-space function of the form factor of the particles, so-called distance distribution function $p(r)$, was also calculated for one of the polymers (Figure 7) by indirect Fourier-transformation of the scattering curve [58]. At 20 °C this resembled the Gaussian bell curve associated with an isotropic spherical shape, with a slight shoulder being attributable to the shell of the core-shell structure. As temperature was increased, $p(r)$ started to diverge from the bell curve and eventually completely it lost that shape as the particles aggregated into different and much larger structures above the C_p temperature (in this case 72°C).

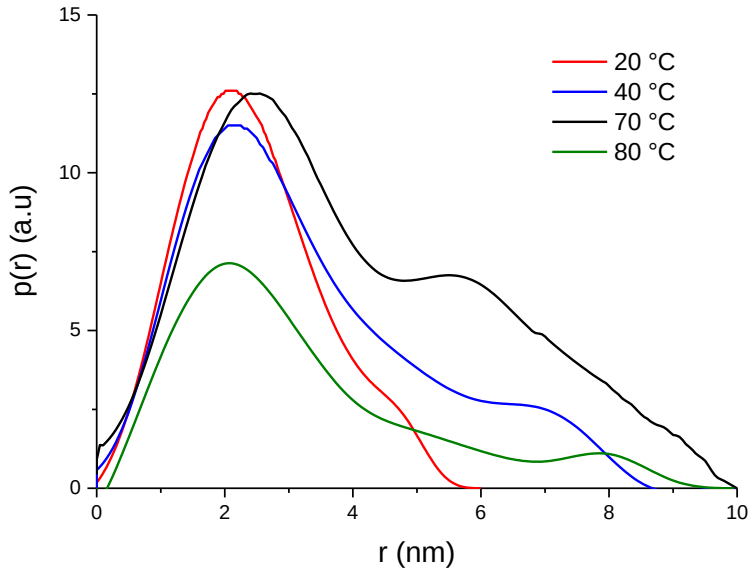

Figure 7: p(r) functions of pEFS8-46 in water solution (20 g/L) at various temperatures

Further elaboration of the data was done by generating Kratky plots ($q^2I(q)$ vs q) to assess the degree of unfolding of the polymers in solution. Unfolded random coil macromolecules would rise to a plateau level for $q^2I(q)$ at large q values, whereas compact, globular macromolecules exhibit a bell curve shape. The Kratky plots from the lower temperature SAXS data confirmed the globular and compact shape of the polymer in water solution (Figure 8a).

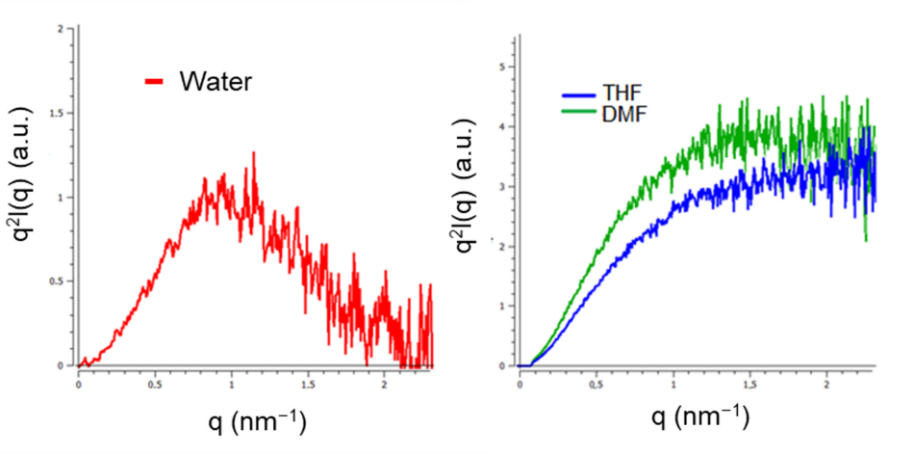

Figure 8: Kratky plots for polymer pEFS8-46 in water (a) and organic solutions (b) (20 g/L) at 20 °C

The effect of an organic solvent on the conformation of the polymer in solution was analyzed for solutions (20 g/L) in THF and DMF. Table 8 shows the radius of gyration R_g of the samples in THF and DMF at 25 °C, as evaluated from Guinier plots in the low q region.

Table 8: Radii of gyration (R_g) of polymers pEFS8-46, pEFS8-135, pEFS13-8 and pEFS13-46 as evaluated by SAXS in THF and DMF solutions

Polymer	***R_g (nm) THF***	***R_g (nm) DMF***
pEFS8-46	2.36 ± 0.02	1.78 ± 0.09
pEFS8-135	1.75 ± 0.07	1.55 ± 0.09
pEFS13-8	1.50 ± 0.08	1.60 ± 0.05
pEFS13-46	2.80 ± 0.06	1.80 ± 0.09

The Kratky plots of analyzed polymers in organic solutions at room temperature were very different from those recorded for the same polymers in water at the same temperature. The Kratky plots of pEFS8-46 in THF and DMF showed an ascending trend until reaching a plateau in the high q region (Figure 8b). This indicated adoption of a non-compact, unfolded or aggregated structure of the polymers in good THF and DMF solvents.

4 Conclusions

New amphiphilic monomers were synthesized and polymerized by ARGET-ATRP to provide the corresponding amphiphilic homopolymers, with an accurate and predetermined control over a wide range of degrees of polymerization with a narrow dispersity. The amphiphilic polymers self-assembled in single-chain nanostructures via self-folding in water solutions, driven by hydrophobic interactions. A compact sphere core-shell system was formed, in which water interacted selectively with the hydrophilic shell. By contrast, the polymers could not self-assemble in THF or DMF solutions and were unfolded in a conventional random coil conformation instead. On increasing temperature to a cloud point temperature, more single-chain nanostructures coalesced into multi-chain (sub)micro-aggregates, that reversibly turned back to the original nanostructures on cooling, according to a LCST-like behavior. Notably, such transition temperatures for several selected polymer solutions were in the range 30–40 °C. Transition temperatures close to human physiological temperature are regarded as more desirable in light of potential application of thermoresponsive polymers in biology and biomedicine contexts.

Acknowledgements

This research was funded by the University of Pisa (Progetti di Ricerca di Ateneo, PRA_2020_27 and PRA_2020_32). This work benefited from the use of the SasView application, originally developed under NSF award DMR-0520547. SasView also contains code developed with funding from the European Union's Horizon 2020 research and innovation programme under the SINE2020 project, grant agreement No 654000.

5 References

[1] O. Altintas, C. Barner-Kowollik, Single chain folding of synthetic polymers by covalent and non-covalent interactions: current status and future perspectives, Macromol. Rapid Commun. 33 (2012) 958–971. https://doi.org/10.1002/marc.201200049.

[2] O. Altintas, T.S. Fischer, C. Barner-Kowollik, Synthetic Methods Toward Single-Chain Polymer Nanoparticles, in: Single-Chain Polym. Nanoparticles, John Wiley & Sons, Ltd, 2017: pp. 1–45. https://doi.org/10.1002/9783527806386.ch1.

[3] H. Frisch, B.T. Tuten, C. Barner-Kowollik, Macromolecular Superstructures: A Future Beyond Single Chain Nanoparticles, Isr. J. Chem. 60 (2020) 86–99. https://doi.org/10.1002/ijch.201900145.

[4] E. Verde-Sesto, A. Arbe, A.J. Moreno, D. Cangialosi, A. Alegría, J. Colmenero, J.A. Pomposo, Single-chain nanoparticles: opportunities provided by internal and external confinement, Mater. Horiz. 7 (2020) 2292–2313. https://doi.org/10.1039/D0MH00846J.

[5] M. Seo, B.J. Beck, J.M.J. Paulusse, C.J. Hawker, S.Y. Kim, Polymeric Nanoparticles via Noncovalent Cross-Linking of Linear Chains, Macromolecules. 41 (2008) 6413–6418. https://doi.org/10.1021/ma8009678.
[6] J. Lu, N. ten Brummelhuis, M. Weck, Intramolecular folding of triblock copolymers via quadrupole interactions between poly(styrene) and poly(pentafluorostyrene) blocks, Chem. Commun. 50 (2014) 6225–6227. https://doi.org/10.1039/C4CC01840K.
[7] E.A. Appel, J. Dyson, J. del Barrio, Z. Walsh, O.A. Scherman, Formation of single-chain polymer nanoparticles in water through host-guest interactions, Angew. Chem. Int. Ed Engl. 51 (2012) 4185–4189. https://doi.org/10.1002/anie.201108659.
[8] I. Berkovich, V. Kobernik, S. Guidone, N.G. Lemcoff, Metal Containing Single-Chain Nanoparticles, in: Single-Chain Polym. Nanoparticles, John Wiley & Sons, Ltd, 2017: pp. 217–257. https://doi.org/10.1002/9783527806386.ch6.
[9] R. Chen, E.B. Berda, 100th Anniversary of Macromolecular Science Viewpoint: Re-examining Single-Chain Nanoparticles, ACS Macro Lett. 9 (2020) 1836–1843. https://doi.org/10.1021/acsmacrolett.0c00774.
[10] Y. Morishima, S. Nomura, T. Ikeda, M. Seki, M. Kamachi, Characterization of Unimolecular Micelles of Random Copolymers of Sodium 2-(Acrylamido)-2-methylpropanesulfonate and Methacrylamides Bearing Bulky Hydrophobic Substituents, Macromolecules. 28 (1995) 2874–2881. https://doi.org/10.1021/ma00112a037.
[11] H. Yamamoto, M. Mizusaki, K. Yoda, Y. Morishima, Fluorescence Studies of Hydrophobic Association of Random Copolymers of Sodium 2-(Acrylamido)-2-methylpropanesulfonate and N-Dodecylmethacrylamide in Water, Macromolecules. 31 (1998) 3588–3594. https://doi.org/10.1021/ma980022u.
[12] T. Terashima, T. Sugita, K. Fukae, M. Sawamoto, Synthesis and Single-Chain Folding of Amphiphilic Random Copolymers in Water, Macromolecules. 47 (2014) 589–600. https://doi.org/10.1021/ma402355v.
[13] Y. Koda, T. Terashima, M. Sawamoto, H.D. Maynard, Amphiphilic/fluorous random copolymers as a new class of non-cytotoxic polymeric materials for protein conjugation, Polym. Chem. 6 (2014) 240–247. https://doi.org/10.1039/C4PY01346H.
[14] E. Martinelli, E. Guazzelli, G. Galli, M.T.F. Telling, G.D. Poggetto, B. Immirzi, F. Domenici, G. Paradossi, Prolate and Temperature-Responsive Self-Assemblies of Amphiphilic Random Copolymers with Perfluoroalkyl and Polyoxyethylene Side Chains in Solution, Macromol. Chem. Phys. 219 (2018) 1800210. https://doi.org/10.1002/macp.201800210.
[15] E. Martinelli, L. Annunziata, E. Guazzelli, A. Pucci, T. Biver, G. Galli, The Temperature-Responsive Nanoassemblies of Amphiphilic Random Copolymers Carrying Poly(siloxane) and Poly(oxyethylene) Pendant Chains, Macromol. Chem. Phys. 219 (2018) 1800082. https://doi.org/10.1002/macp.201800082.
[16] E. Guazzelli, E. Masotti, T. Biver, A. Pucci, E. Martinelli, G. Galli, The self-assembly over nano- to submicro-length scales in water of a fluorescent julolidine-labeled amphiphilic random terpolymer, J. Polym. Sci. Part Polym. Chem. 56 (2018) 797–804. https://doi.org/10.1002/pola.28955.
[17] K. Matsumoto, T. Terashima, T. Sugita, M. Takenaka, M. Sawamoto, Amphiphilic Random Copolymers with Hydrophobic/Hydrogen-Bonding Urea Pendants: Self-Folding Polymers in Aqueous and Organic Media, Macromolecules. 49 (2016) 7917–7927. https://doi.org/10.1021/acs.macromol.6b01702.
[18] Y. Kimura, T. Terashima, M. Sawamoto, Self-Assembly of Amphiphilic Random Copolyacrylamides into Uniform and Necklace Micelles in Water, Macromol. Chem. Phys. 218 (2017) 1700230. https://doi.org/10.1002/macp.201700230.
[19] T. Terashima, Controlled Self-Assembly of Amphiphilic Random Copolymers into Folded Micelles and Nanostructure Materials, J. Oleo Sci. 69 (2020) 529–538. https://doi.org/10.5650/jos.ess20089.

[20] Y. Koda, T. Terashima, M. Sawamoto, Multimode Self-Folding Polymers via Reversible and Thermoresponsive Self-Assembly of Amphiphilic/Fluorous Random Copolymers, Macromolecules. 49 (2016) 4534–4543. https://doi.org/10.1021/acs.macromol.6b00998.
[21] G. Hattori, M. Takenaka, M. Sawamoto, T. Terashima, Nanostructured Materials via the Pendant Self-Assembly of Amphiphilic Crystalline Random Copolymers, J. Am. Chem. Soc. 140 (2018) 8376–8379. https://doi.org/10.1021/jacs.8b03838.
[22] Y. Hirai, T. Terashima, M. Takenaka, M. Sawamoto, Precision Self-Assembly of Amphiphilic Random Copolymers into Uniform and Self-Sorting Nanocompartments in Water, Macromolecules. 49 (2016) 5084–5091. https://doi.org/10.1021/acs.macromol.6b01085.
[23] S. Imai, Y. Hirai, C. Nagao, M. Sawamoto, T. Terashima, Programmed Self-Assembly Systems of Amphiphilic Random Copolymers into Size-Controlled and Thermoresponsive Micelles in Water, Macromolecules. 51 (2018) 398–409. https://doi.org/10.1021/acs.macromol.7b01918.
[24] M. Shibata, M. Matsumoto, Y. Hirai, M. Takenaka, M. Sawamoto, T. Terashima, Intramolecular Folding or Intermolecular Self-Assembly of Amphiphilic Random Copolymers: On-Demand Control by Pendant Design, Macromolecules. 51 (2018) 3738–3745. https://doi.org/10.1021/acs.macromol.8b00570.
[25] Y. Ommura, S. Imai, M. Takenaka, M. Ouchi, T. Terashima, Selective Coupling and Polymerization of Folded Polymer Micelles to Nanodomain Self-Assemblies, ACS Macro Lett. 9 (2020) 426–430. https://doi.org/10.1021/acsmacrolett.0c00013.
[26] C. Nagao, M. Sawamoto, T. Terashima, Molecular imprinting on amphiphilic folded polymers for selective molecular recognition in water, J. Polym. Sci. 58 (2020) 215–224. https://doi.org/10.1002/pol.20190003.
[27] J.A. Pomposo, I. Perez-Baena, F. Lo Verso, A.J. Moreno, A. Arbe, J. Colmenero, How Far Are Single-Chain Polymer Nanoparticles in Solution from the Globular State?, ACS Macro Lett. 3 (2014) 767–772. https://doi.org/10.1021/mz500354q.
[28] A.P.P. Kröger, J.M.J. Paulusse, Single-chain polymer nanoparticles in controlled drug delivery and targeted imaging, J. Controlled Release. 286 (2018) 326–347. https://doi.org/10.1016/j.jconrel.2018.07.041.
[29] T. Terashima, T. Mes, T.F.A. De Greef, M.A.J. Gillissen, P. Besenius, A.R.A. Palmans, E.W. Meijer, Single-Chain Folding of Polymers for Catalytic Systems in Water, J. Am. Chem. Soc. 133 (2011) 4742–4745. https://doi.org/10.1021/ja2004494.
[30] M. Artar, T. Terashima, M. Sawamoto, E.W. Meijer, A.R.A. Palmans, Understanding the catalytic activity of single-chain polymeric nanoparticles in water, J. Polym. Sci. Part Polym. Chem. 52 (2014) 12–20. https://doi.org/10.1002/pola.26970.
[31] M. Artar, E.R.J. Souren, T. Terashima, E.W. Meijer, A.R.A. Palmans, Single Chain Polymeric Nanoparticles as Selective Hydrophobic Reaction Spaces in Water, ACS Macro Lett. 4 (2015) 1099–1103. https://doi.org/10.1021/acsmacrolett.5b00652.
[32] Y. Azuma, T. Terashima, M. Sawamoto, Self-Folding Polymer Iron Catalysts for Living Radical Polymerization, ACS Macro Lett. 6 (2017) 830–835. https://doi.org/10.1021/acsmacrolett.7b00498.
[33] J. Chen, E.S. Garcia, S.C. Zimmerman, Intramolecularly Cross-Linked Polymers: From Structure to Function with Applications as Artificial Antibodies and Artificial Enzymes, Acc. Chem. Res. 53 (2020) 1244–1256. https://doi.org/10.1021/acs.accounts.0c00178.
[34] A. Bartolini, P. Tempesti, C. Resta, D. Berti, J. Smets, Y.G. Aouad, P. Baglioni, Poly(ethylene glycol)-graft-poly(vinyl acetate) single-chain nanoparticles for the encapsulation of small molecules, Phys. Chem. Chem. Phys. 19 (2017) 4553–4559. https://doi.org/10.1039/C6CP07967A.
[35] J.H. Ko, A. Bhattacharya, T. Terashima, M. Sawamoto, H.D. Maynard, Amphiphilic fluorous random copolymer self-assembly for encapsulation of a fluorinated agrochemical, J. Polym. Sci. Part Polym. Chem. 57 (2019) 352–359. https://doi.org/10.1002/pola.29187.

[36] C.A. Sanders, S.R. George, G.A. Deeter, J.D. Campbell, B. Reck, M.F. Cunningham, Amphiphilic Block-Random Copolymers: Self-Folding Behavior and Stabilizers in Emulsion Polymerization, Macromolecules. 52 (2019) 4510–4519. https://doi.org/10.1021/acs.macromol.9b00519.
[37] S.-Y. Huang, C.-C. Cheng, Spontaneous Self-Assembly of Single-Chain Amphiphilic Polymeric Nanoparticles in Water, Nanomaterials. 10 (2020) 2006. https://doi.org/10.3390/nano10102006.
[38] Y. Kimura, M. Ouchi, T. Terashima, Folded amphiphilic homopolymer micelles in water: uniform self-assembly beyond amphiphilic random copolymers, (2020). https://doi.org/10.1039/d0py00685h.
[39] Y. Kimura, T. Terashima, Morphology transition of amphiphilic homopolymer self-assemblies in water triggered by pendant design and chain length, Eur. Polym. J. 139 (2020) 110001. https://doi.org/10.1016/j.eurpolymj.2020.110001.
[40] S. Hvilsted, The pentafluorostyrene endeavours with atom transfer radical polymerization—quo vadis?, Polym. Int. 63 (2014) 814–823. https://doi.org/10.1002/pi.4613.
[41] E. Martinelli, G. Pelusio, B.R. Yasani, A. Glisenti, G. Galli, Surface Chemistry of Amphiphilic Polysiloxane/Triethyleneglycol-Modified Poly(pentafluorostyrene) Block Copolymer Films Before and After Water Immersion, Macromol. Chem. Phys. 216 (2015) 2086–2094. https://doi.org/10.1002/macp.201500221.
[42] E. Martinelli, S.D. Hill, J.A. Finlay, M.E. Callow, J.A. Callow, A. Glisenti, G. Galli, Amphiphilic modified-styrene copolymer films: Antifouling/fouling release properties against the green alga Ulva linza, Prog. Org. Coat. C (2016) 235–242. https://doi.org/10.1016/j.porgcoat.2015.10.005.
[43] K.T. Powell, C. Cheng, K.L. Wooley, Complex Amphiphilic Hyperbranched Fluoropolymers by Atom Transfer Radical Self-Condensing Vinyl (Co)polymerization, Macromolecules. 40 (2007) 4509–4515. https://doi.org/10.1021/ma0628937.
[44] J.W. Bartels, C. Cheng, K.T. Powell, J. Xu, K.L. Wooley, Hyperbranched Fluoropolymers and their Hybridization into Complex Amphiphilic Crosslinked Copolymer Networks, Macromol. Chem. Phys. 208 (2007) 1676–1687. https://doi.org/10.1002/macp.200700104.
[45] P.M. Imbesi, N.V. Gohad, M.J. Eller, B. Orihuela, D. Rittschof, E.A. Schweikert, A.S. Mount, K.L. Wooley, Noradrenaline-functionalized hyperbranched fluoropolymer-poly(ethylene glycol) cross-linked networks as dual-mode, anti-biofouling coatings, ACS Nano. 6 (2012) 1503–1512. https://doi.org/10.1021/nn204431m.
[46] B.H. Tan, H. Hussain, Y. Liu, C.B. He, T.P. Davis, Synthesis and Self-Assembly of Brush-Type Poly[poly(ethylene glycol)methyl ether methacrylate]-block-poly(pentafluorostyrene) Amphiphilic Diblock Copolymers in Aqueous Solution, Langmuir. 26 (2010) 2361–2368. https://doi.org/10.1021/la902816b.
[47] B.H. Tan, H. Hussain, K.C. Chaw, G.H. Dickinson, C.S. Gudipati, W.R. Birch, S.L.M. Teo, C. He, Y. Liu, T.P. Davis, Barnacle repellent nanostructured surfaces formed by the self-assembly of amphiphilic block copolymers, Polym. Chem. 1 (2010) 276–279. https://doi.org/10.1039/B9PY00332K.
[48] F. Zuppardi, F.R. Chiacchio, R. Sammarco, M. Malinconico, G. Gomez d'Ayala, P. Cerruti, Fluorinated oligo(ethylene glycol) methacrylate-based copolymers: Tuning of self assembly properties and relationship with rheological behavior, Polymer. 112 (2017) 169–179. https://doi.org/10.1016/j.polymer.2017.01.080.
[49] F. Zuppardi, M. Malinconico, F. D'Agosto, G.G. D'Ayala, P. Cerruti, Well-Defined Thermo-Responsive Copolymers Based on Oligo(Ethylene Glycol) Methacrylate and Pentafluorostyrene for the Removal of Organic Dyes from Water, Nanomaterials. 10 (2020) 1779. https://doi.org/10.3390/nano10091779.
[50] D. Szweda, R. Szweda, A. Dworak, B. Trzebicka, Thermoresponsive poly[oligo(ethylene glycol) methacrylate]s and their bioconjugates - Synthesis and solution behavior, Polimery. 62 (2017) 298–310. https://doi.org/10.14314/polimery.2017.298.

[51] A. Bordat, T. Boissenot, J. Nicolas, N. Tsapis, Thermoresponsive polymer nanocarriers for biomedical applications, Adv. Drug Deliv. Rev. 138 (2019) 167–192. https://doi.org/10.1016/j.addr.2018.10.005.
[52] C. Pelosi, E. Guazzelli, M. Calosi, L. Bernazzani, M.R. Tiné, C. Duce, E. Martinelli, Investigation of the LCST-Thermoresponsive Behavior of Novel Oligo(Ethylene Glycol)-Modified Pentafluorostyrene Homopolymers, Appl. Sci. 11 (2021) 2711. https://doi.org/10.3390/app11062711.
[53] A.K. Brewer, A.M. Striegel, Characterizing the size, shape, and compactness of a polydisperse prolate ellipsoidal particle via quadruple-detector hydrodynamic chromatography, The Analyst. 136 (2011) 515–519. https://doi.org/10.1039/C0AN00738B.
[54] H.-U. ter Meer, W. Burchard, W. Wunderlich, Quasi-elastic light scattering from polymethylmethacrylate in a good and a theta solvent, Colloid Polym. Sci. 258 (1980) 675–684. https://doi.org/10.1007/BF01384359.
[55] D.-M. Smilgies, E. Folta-Stogniew, Molecular weight–gyration radius relation of globular proteins: a comparison of light scattering, small-angle X-ray scattering and structure-based data, J. Appl. Crystallogr. 48 (2015) 1604–1606. https://doi.org/10.1107/S1600576715015551.
[56] N. Sanson, F. Bouyer, M. Destarac, M. In, C. Gérardin, Hybrid Polyion Complex Micelles Formed from Double Hydrophilic Block Copolymers and Multivalent Metal Ions: Size Control and Nanostructure, Langmuir. 28 (2012) 3773–3782. https://doi.org/10.1021/la204562t.
[57] A. Guinier, G. Fournet, Small-Angle Scattering of X-Rays, John Wiley and Son, New York, 1955.
[58] R. Mittelbach, O. Glatter, Direct Structure Analysis of Small-Angle Scattering Data from Polydisperse Colloidal Particles, J. Appl. Crystallogr. 31 (1998) 600–608. https://doi.org/10.1107/S0021889898002209.